EUROPEAN HEMATOLOGY ASSOCIATION
haematologica
Journal of the European Hematology Association

Factor H interfers with the adhesion of sickle red cells to vascular endothelium: a novel disease modulating molecule

by Elisabetta Lombardi, Alessandro Matte, Antonio M. Risitano, David Ricklin, John D. Lambris, Denise De Zanet, Sakari T. Jokiranta, Nicola Martinelli, Cinzia Scambi, Gianluca Salvagno, Zeno Bisoffi, Chiara Colato, Angela Siciliano, Oscar Bortolami, Mario Mazzuccato, Francesco Zorzi, Luigi De Marco, and Lucia De Franceschi

Haematologica 2019 [Epub ahead of print]

Citation: Elisabetta Lombardi, Alessandro Matte, Antonio M. Risitano, David Ricklin, John D. Lambris, Denise De Zanet, Sakari T. Jokiranta, Nicola Martinelli, Cinzia Scambi, Gianluca Salvagno, Zeno Bisoffi, Chiara Colato, Angela Siciliano, Oscar Bortolami, Mario Mazzuccato, Francesco Zorzi, Luigi De Marco, and Lucia De Franceschi. Factor H interfers with the adhesion of sickle red cells to vascular endothelium: a novel disease modulating molecule.
Haematologica. 2019; 104:xxx
doi:10.3324/haematol.2018.198622

Factor H interferes with the adhesion of sickle red cells to vascular endothelium: a novel disease modulating molecule

Elisabetta Lombardi,[1*] Alessandro Matte,[2*] Antonio M. Risitano,[3] Daniel Ricklin,[4] John D. Lambris,[5] Denise De Zanet,[1, 6] Sakari T. Jokiranta,[7] Nicola Martinelli,[2] Cinzia Scambi[2], Gianluca Salvagno,[8] Zeno Bisoffi,[9,10] Chiara Colato,[10] Angela Siciliano,[2] Oscar Bortolami,[11] Mario Mazzuccato,[1] Francesco Zorzi, [2] Luigi De Marco,[1, 12#] Lucia De Franceschi[2]

[1]Dept of Translational Research, National Cancer Center, Aviano, Italy; [2]Dept of Medicine, University of Verona-AOUI Verona, Verona; Italy; [3]Hematology, Dept of Clinical Medicine and Surgery, Federico II University, Naples; Italy; [4]Molecular Pharmacy Group, Dep of Pharmaceutical Sciences, University of Basel, Basel, Switzerland; [5]Dept of Pathology and Laboratory Medicine, Perelman School of Medicine, University of Pennsylvania, Philadelphia, PA; USA; [6]Polytechnic Department of Engineering and Architecture, University of Udine, Italy; [7]Research Programs Unit, Immunobiology, University of Helsinki; and United Medix Laboratories, Helsinki, Finland; [8]Laboratory of Clinical Biochemistry, Department of Life and Reproduction Sciences, University of Verona, Verona, Italy; [9]Centre of Tropical Diseases, Sacro Cuore-Don Calabria Hospital Negrar, Verona, Italy; [10]Dept of Diagnostics and Public Health, University of Verona-AOUI Verona, Verona; Italy; [11]Unit of Epidemiology and Medical Statistics, Dept of Diagnostic & Public Health, University of Verona;[12]Dept of Molecular Medicine, The Scripps Research Institute, 10550 N Torrey Pines Rd, La Jolla CA 92037 USA

Key words: Mac-1, RBC adhesion, complement, P-selectin, SCD
Running title: Complement is involved in sickle red cell adhesion
Words count: 3919

Corresponding Author:
Lucia De Franceschi, MD
Policlinico GB Rossi; P. Le L. Scuro, 10; 37134 Verona; Italy;
Phone: +390458124401; FAX: +390458027473; E-mail: lucia.defranceschi@univr.it
*E.L. and A.M equally contributed to this study; #L.D.M.: co-last author

ABSTRACT

Sickle cell disease is an autosomal recessive genetic red cell disorder with worldwide distribution. Growing evidence suggests a possible involvement of complement activation in the severity of sickle cell clinical complication. Here, we found activation of the alternative complement pathway with microvascular deposition of C5b-9 on skin biopsies from sickle cell disease patients. This was also supported by sickle red cell membrane the deposition of C3b on sickle red cell membranes, which is locally promoted by the exposure of phosphatidylserine. In addition, we showed for the first time a peculiar “stop-and-go” motion of SCD RBCs on TNF-α activated vascular endothelial surfaces.

Using the C3b/iC3b binding plasma protein Factor-H as an inhibitor of C3b cell-cell interactions, we found that Factor-H and Factor-H 19-20 domains prevent the adhesion of sickle red cells to the endothelium, normalizing speed transition times of red cells on inflammatory activated endothelium. We have firstly documented that FH acts by preventing the adhesion of sickle red cells to P-selectin and/or the receptor Mac-1 receptor (CD11b/CD18), supporting the activation of the alternative pathway of complement as an additional mechanism in the pathogenesis of acute sickle cell related vaso-occlusive crisis. Our data provide a rationale for further investigation of the potential contribution of Factor-H and other modulators of the alternative complement pathway with potential implications to the treatment of sickle cell disease.

INTRODUCTION

Sickle cell disease (SCD; OMIM # 603903) is an autosomal recessive genetic red blood cell (RBC) disorder with worldwide distribution. SCD results from a point mutation (β^S, 6V) in codon 6 of the β-globin gene where the insertion of valine in place of glutamic acid leads to the production of a defective form of hemoglobin, termed hemoglobin S (HbS) (1-3). Pathophysiological studies have shown that intravascular sickling in capillaries and small vessels leads to vaso-occlusion and impaired blood flow. Vaso-occlusive events in the microcirculation result from a complex and only partially known scenario involving the interactions between different cell types. These cells include dense, dehydrated sickle cells, reticulocytes, abnormally activated endothelial cells, leukocytes and platelets.(1-4) Plasma factors such as coagulation system cytokines and oxidized pro-inflammatory lipids may also be involved. In addition, the cyclic polymerization-depolymerization events promote RBC membrane oxidation and reduce RBC survival in the peripheral circulation(1, 5, 6). The resulting increase in free hemoglobin and free heme, a consequence of the saturation of the physiologic system and local reduction of nitric oxide bioavailability, leads to a pro-coagulant state with increased risk of thrombotic events (2, 3, 7-10). All this evidence indicates that sickle cell vasculopathy is a crucial player in RBC adhesion events and in the generation of acute vaso-occlusive events in SCD patients.

Although progress has been made in recent decades concerning the pathogenesis of SCD, the molecular events involved in these processes are still only partially delineated. Whereas, a key role for complement activation has been highlighted in chronic inflammatory processes characterized by hemolysis and inflammatory vasculopathy such as atypical hemolytic uremic syndromes (aHUS) and paroxysmal nocturnal hemoglobinuria (PNH) (11-14), the involvement of complement in SCD has been less extensively explored. Previous studies have revealed (i) an activation of the alternative complement pathway (AP) of complement activation in SCD patients; (ii) a reduction in the activating proteases factor B and D, modulating complement activation; (iii) a decrease in the plasma levels of FH, the major soluble regulator of AP activation; and (iv) increased deposition of the

complement opsonin C3b on RBC exposing phosphatidylserine (PS) (15-22). Preliminary data from a mouse model for SCD suggest a possible role for complement activation in the generation of vaso-occlusive crisis (VOCs), as an additional disease mechanism contributing to the severity of acute clinical manifestations related to SCD (23, 24).

Because of its potential detrimental effects on host cells, the AP is finely regulated by membrane-bound and soluble regulators. Circulating FH plays a particularly important role, since this regulator not only binds to C3b and prevents the formation of C3b convertases, but it is also able to recognize self-associated molecular patterns such as sialic acid and glycosaminoglycans present on the membranes of most healthy cells (25-27). Any interference with this recognition process, resulting from either polymorphisms or blocking antibodies against FH, may have severe pathological consequences as described for aHUS and other complement mediated disorders (28).

Here, we found that sickle RBCs are characterized by membrane deposition of C3b, which acts as a marker for the activation of the AP on sickle RBCs. We sought to determine whether C3b depositions on RBCs might possibly stimulate VOCs by favoring cell-cell interactions. Indeed, we now demonstrate for the first time a peculiar *ex vivo* motion profile ("stop-and-go" behavior) of SCD red cells during their transit on vascular endothelial surfaces, a motion that prolongs their transit of the vascular endothelial surface and promotes the adhesion of sickle RBCs. We show that FH and its 19-20 domain (29, 30), which primarily targets C3b, prevent the adhesion of sickle RBCs to the endothelium. We further documented that FH acts by preventing the adhesion of sickle RBCs to P-selectin and/or the receptor Mac-1(CD11b/CD18). Our data provide a rationale for further investigation of FH and other modulators of the alternative complement pathway as novel disease modifying molecules with potential implications for the treatment of the clinical manifestations of SCD.

METHODS

Study design

We studied SCD subjects (*n*=29; 26 SS and 3 $S\beta^0$) subjects referred to the Department of Medicine, University of Verona and Azienda Ospedaliera Integrata of

Verona (Italy), from January 2012 to January 2017. SCD patients were evaluated at steady state, and none of them had been on either on hydroxyurea or a transfusion regimen during the 6 months immediately prior to our analysis. Healthy controls were matched by age, sex and ethnic background. The study was approved by the Ethical Committee of the Azienda Ospedaliera Integrata of Verona (Italy) and informed consent was obtained from patients and healthy controls (Ethical approval FGRF13IT). Table 1 shows the demographic characteristics of both the healthy and SCD subjects studied. Biochemical and hematologic parameters as well as plasma levels of C3 and C4 were determined according to clinical and laboratory standards at the Laboratory of Medicine, University of Verona and Azienda Ospedaliera Integrata of Verona (Italy). Plasma C5a (EIA Quidel Corp., San Diego, CA; USA), plasma VCAM-1 (Invitrogen, Carlsbad, CA; USA) and serum FH (Hycult Biotech, Uden, The Netherlands) were determined by ELISA, according to manufacturers' protocols (31).

Evaluation of C5b-9 complement deposition on fixed skin biopsy

Skin punch biopsies were carried out on the volar surface of the left arm on apparently normal skin. The samples were paraffin-embedded and examined by routine hematoxylin and eosin (H and E); they also were used to estimate the presence, within the microvasculature (32). Details on Immunofluorescent and Immunohistochemical staining assays are reported in Supplemental Methods (32-34).

Measurements of phosphatidylserine+ and C3d+ RBCs

Phosphatidylserine (PS)-positive cells were detected as previously reported (35-37). Details are reported in Supplemental Methods.

RBCs adhesion assay

The real time adhesion of RBCs collected from healthy and SCD subjects on inactive or activated endothelium (in the absence or presence of TNF-α, respectively) was performed as previously reported (38-40) with or without FH or FH19-20 or FH68 domains (41). Details are reported in Supplemental Methods.

Development of an algorithm to determine RBC transit and flux trajectory

Details on the algorithm to determine RBC transit and flux trajectory are reported in Supplemental Methods.

P-selectin and Mac-1 expression *in vitro* in vascular endothelial cells

Details on immunoblot (42) and cytofluorimetric analysis are reported on Supplemental Methods.

Statistical analysis

All calculations were performed using the IBM SPSS 20.0 (IBM Inc., Armonk, NY) statistical package. The level of aggregation was expressed as median values with the minimum-maximum range and shown by means of either dot or box plots. Data were analyzed with non-parametric tests, the Mann-Whitney *U* test for unpaired samples and Wilcoxon signed-rank test for paired samples. A value of $P<0.05$ was considered statistically significant.

RESULTS

SCD patients show activation of the AP and increased C3d+ RBCs

Untreated SCD subjects at steady state were studied. As shown in Table 1, reduced hemoglobin, increased reticulocyte counts and plasma LDH, all signs of chronic hemolytic anemia were observed (Table 1). In SCD patients, we also found a significant increase of plasma CRP and sVCAM-1 levels, indicating the presence of chronic inflammatory vasculopathy in agreement with previous reports (2, 3, 9, 43). Serum C3 and C4 were similar in healthy and SCD subjects (data not shown); whereas levels of the complement activation fragment C5a were significantly elevated in SCD patients when compared to healthy individuals (Fig. 1A); statistical analyses were performed to exclude the possible contribution of confounding factors such as gender or smoking status. Our finding is consistent with previous reports, and confirms the substantial complement activation in SCD patients, likely via the AP (15-22).

Since studies in aHUS have shown that skin biopsy might be a feasible tool for documenting AP activation by C5b-9 vascular deposition (32), we obtained skin biopsies from SCD patients at steady state. We considered skin to be an interesting window of observation in SCD, since (i) it might be involved in clinical manifestation of SCD, such as leg ulcers; and (ii) it has been widely used in SCD mouse models to functionally characterize the microvasculature (44-47). As shown in Fig. 1B, we observed microvascular intense, focal granular deposition of C5b-9 in small vessels throughout the dermis of SCD patients. This pattern is similar to that reported in skin biopsies from patients with aHUS, which is a thrombotic microangiopathy related to complement dysfunction (32). No deposition of C5b9 was observed in skin from

healthy controls (Fig. 1SA-B). Co-localization of C59b deposits and CD31-positive skin vessels was confirmed by immunohistochemical staining only in the skin biopsies from SCD patients (Fig. 1C, Fig. 2SA-B).

Taken together, our data indicate an activation of AP in SCD, with possible involvement of complement in SCD vasculopathy and in related cellular adhesion events.

To understand whether AP activation occurs directly on sickle RBCs, we measured the amounts of circulating RBCs carrying C3-derived opsonins by detecting the presence of the common C3d fragment (11, 12). As shown in Fig. 1D, higher amounts of C3d+ RBC were found in SCD patients in the steady state when compared to healthy subjects (representative scatter-plots are shown in Fig. 3S). This fraction further increased in a subgroup of SCD patients during acute pain crisis (SS steady state 2.5$\pm$0.8% *vs* SS pain-crisis: 6.1$\pm$0.7 % $P<0.02$; $n=10$), in agreement with an observation by Mold et al. (18). Since a previous report has linked the activation of AP with deposition of C3 opsonins to the exposure of PS on SCD RBC surfaces, we evaluated the percentage of PS+ RBCs in our SCD patients (17). Indeed, we found increased percentage of PS+ RBCs in SCD patients compared to healthy subjects in agreement with previous studies (35, 36) (Fig. 1E). In contrast to PNH, in which opsonization leads to rapid lysis of affected RBCs (11, 12), the presence of functional membrane regulators on SCD erythrocytes allowed a low level of C3-fragment deposition, which might also be considered as marker of complement activation on sickle RBCs. We therefore reasoned that the presence of C3b, iC3b or C3dg may function as a site of adhesion of SCD RBCs to activated vascular endothelial surface, which may carry ligands for C3 fragments, such as Mac-1 or P-selectin (48, 49). To study this event, we used the C3b and iC3b binding plasma protein FH as an inhibitor (25-27) and saw no significant differences in FH serum levels (AA median: 841 (range 616-1528) µg/mL *vs* SCD median: 980 (741-1301) µg/mL; NS) between healthy and SCD subjects.

FH prevents the adhesion of sickle RBCs to TNF-α activated vascular endothelium

We performed an *ex vivo* adhesion assay using TNF-α- activated vascular endothelial cells and monitored in real time the adhesion of RBCs collected from healthy and SCD subjects to inactive (no TNF-α) or activated endothelium (plus

TNF-α) as previously described (38-40). Consistent with the literature, we observed significantly increased adhesion of SCD RBCs to TNF-α-activated endothelium when compared to normal RBCs (Fig. 2A, online video 1). We next investigated the effect of FH on the adhesion of healthy or SCD RBCs to activated vascular endothelium. The dose-response curve with FH showed a significant reduction in RBC adhesion at concentrations $\geq$ 9 nM (Fig. 2B). This was more pronounced in SCD RBCs compared to healthy RBCs (Fig. 2B). Therefore, we expanded the tests to include a larger number of SCD patients using FH concentrations of 9 or 18 nM; as expected, reduced adhesion of SCD RBCs to the vascular endothelium was observed in presence of either 9 nM or 18 nM FH (Fig. 3A). Previous studies have identified two major regions on FH (i.e., domains 6-8 and 19-20) as the putative sites of interaction with the cell surface constituents such as glycosaminoglycans; furthermore, domains 19-20 are also responsible for binding to sialic acids or C3d-containing deposits (29). We therefore evaluated whether any of these segments would have activity similar to that of full-length FH.

Perfusion experiments performed on TNF-α-activated endothelium demonstrated that, like intact FH, FH19-20 (18 nM) strongly prevented the adhesion of sickle RBCs to the surface of TNF-α-activated vascular endothelium. Conversely, FH6-8 showed a trend toward a reduction in RBC adhesion that did not reach statistical significance (Fig. 3B). Our data indicate that the FH prevents sickle cell adhesion to the activated endothelium through its interaction with cell-surface sialic acids and C3b/iC3b found on the surface of pathological RBCs (Fig. 3B).

FH and the FH19-20 domain normalize the sickle RBC trajectory and transverse velocity on TNF-α activated vascular endothelium

We then developed a new algorithm for RBCs to analyze their trajectory and transverse velocity, the velocity component perpendicular to the flow direction of the RBCs during their transit in the flowing chamber. The trajectory of each sickle RBC appeared irregular in space and was not uniform in time, especially when compared to that of healthy RBCs (Fig. 4A, B). This observation was based on the high transverse displacement and the presence of frequent stop-and-go motion that characterized the sickle RBCs transit of the activated vascular endothelium. The transverse velocity is a parameter that is correlated with the disturbed movement of a particle. Therefore, the path of healthy RBCs appears to be more regular, uniform,

and parallel to the flow (Fig. 4A, online video 2). Thus, healthy RBCs crossed the field of view more rapidly than did sickle RBCs (0.8-1.2 vs 1.7-2 sec, respectively; $p<0.05$). In the presence of FH, sickle RBCs regularized their trajectory (Fig. 4C), reducing their transverse velocity up to 7.71 ± 6.7 µm/second (average decrease of 81.13% *vs* vehicle-treated sickle RBCs). The same behavior appeared in sickle RBCs treated only with the FH 19-20 domain alone (Fig. 4D), with the transverse speed being 6.56 ± 5.6 µm/second (an average decrease of 83.94% vs vehicle-treated sickle RBCs). When the particle kinematics were quantified (Fig. 3E), we found that sickle RBCs exhibited an absolute value for the instantaneous transverse speed of 40.86 ± 27.6 µm/second, whereas for healthy cells the value was only 5.64 ± 4.9 µm/second (a difference of 86.20%). When healthy cells were compared to either FH or FH19-20-treated sickle RBCs, the absolute values for instantaneous transverse speed decreased significantly, reaching values similar to those observed for healthy RBCs.

Anti-P-selectin and anti-Mac-1 antibodies prevent adhesion of SCD RBCs to TNF-α activated vascular endothelial surface

To better understand the possible binding proteins that are important for adhesion of C3b/iC3b+ SCD red cells, we then evaluated the effects of anti-P-selectin antibody or anti-Mac-1 antibodies on the adhesion of SCD to TNF-α activated vascular endothelium. We chose these two molecules for the following reasons: (i) they are both modulated in endothelial cells (2, 50-55); (ii) P-selectin has been reported to bind C3b present on the membranes of circulating cells such as platelets (56); and (iii) Mac-1 is a well-known receptor for iC3b, and potentially C3dg associated with the cell membrane (25). In addition, P-selectin has been reported to bind RBCs, targeting red cell plasma-membrane sialic acid, whereas the presence of a Mac-1 binding site on RBC membranes is still under investigation (29, 48, 51, 57). In our model, the expression of P-selectin and Mac-1 was significantly increased in TNF-α activated vascular endothelium when compared to vehicle treated cells (Fig. 4SA). Both anti-P-selectin and anti-Mac1 antibodies prevented the adhesion of sickle RBCs to the activated vascular endothelium (Fig. 5A). Whereas, the effect of the anti-P-selectin Ab on RBC adhesion may be mediated through an interference with two different targets (i.e., iC3b and/or sialic acid), the interplay between Mac-1 and iC3b deposited on sickle RBCs is considered to be more selective (25, 58). The anti-

adhesive effect of the anti-Mac-1 Ab was more pronounced than that of the anti-P-selectin Ab, but the difference was not statistically significant. No effect on the adhesion of sickle RBCs was documented in presence of a control Ab (Fig. 4SB). Collectively, these findings indicate that C3b/iC3b is deposited on sickle RBC membranes as a new ligand, bridging sickle RBCs to the activated vascular endothelial surface through binding to the pro-adhesive molecules: P-selectin and/or Mac-1.

DISCUSSION

Here, we confirm the activation of AP in SCD and we demonstrate, for the first time, cutaneous vascular deposition of C5b-9, supporting the involvement of complement in the microvascular injury associated with SCD.

We then show that the activation of the AP results in C3 split-fragments being bound to the sickle RBC surface, thereby contributing to the adhesion of RBCs to the inflammatory activated vascular endothelial surface. Notably, decoration of erythrocytes with C3 opsonins was more evident in patients undergoing VOCs, further supporting the involvement of complement in microvascular injury in SCD. Since sickle RBCs, in contrast to PNH RBCs, still contain the functional complement regulators CD55 and CD59, PS-mediated complement activation may allow for a certain degree of opsonization without inducing hemolysis. This situation would lead to the observed accumulation of C3d-containing opsonins (i.e., C3b, iC3b, C3dg), which have all been associated with cell interaction and signaling functions (59). Thus, we propose that C3 split-fragments on RBCs might favor cell-cell interaction, as supported by previous observations of reduced RBCs-cells interactions in mice genetically lacking the C3 complement fraction (51, 60).

We also demonstrate here that FH prevents the adhesion of sickle RBCs and normalizes their trajectory and tranverse velocity of sickle erythrocytes on TNF-α-activated vascular endothelial surfaces through a mechanism involving P-selectin and/or Mac-1 as pro-adhesion molecule(s). FH that binds to C3b/iC3b molecules present on cell surfaces and inhibits ACP. The algorithm developed within the present study allowed us to go farther in describing RBC adhesion to the endothelial surface. Indeed, we show that SCD RBCs adhere to endothelial cells with a peculiar dynamic behavior not shown by healthy RBCs. The stop-and-go profile of sickle

RBCs contributes to their irregular trajectory of sickle RBCs during their transit on the vascular endothelial surface. This slow and irregular movement clearly affects the speed transition time of sickle RBCs when compared to healthy controls, possibly contributing to the reduction in blood flow in the microcirculation that generally characterizes the early phase of acute VOCs (1, 5, 61-63). It is thus conceivable that our flow-based methodology could have a positive impact on the monitoring therapy of SCD. Both FH and its FH19-20 segment normalized the transit of sickle RBCs across the TNF-α activated vascular endothelial surface, abolishing the “stop-and-go” behavior of sickle RBCs. This effect is of great importance because the transition time of sickle RBCs in microcirculation is critically related to the HbS polymerization time and the generation of dense, dehydrated RBCs, which contribute to the development of the acute clinical manifestation of SCD (1, 10). It is important to note that FH appears to exert a non-canonical function in preventing cell adhesion. This complement regulator typically inhibits complement activation via the AP by accelerating the decay of C3 convertases and by mediating the degradation of C3b to iC3b and C3dg via the plasma protease Factor I. Since our experiments have been performed using purified cells in the absence of plasma or serum, Factor I and the components involved in convertase formation cannot be involved in the observed effects. Rather, FH appears to interfere directly with cell-cell interaction events between sickle RBCs and endothelial cells.

To further identify the mechanism of complement opsonin-mediated adhesion and the role of FH as an anti-adhesive molecule for SCD RBCs, we pre-coated vascular endothelial cells with either anti-P-selectin or anti-Mac-1 Abs. Both surface molecules are expressed on activated vascular endothelial cells and have been associated with opsonin interactions. Mac-1 is well-established as a functionally important receptor for iC3b that contributes to phagocytosis and cell activation. Whereas, the interplay of complement with P-selectin is less well described, several reports showed interactions between C3b and P-selectin (56, 64, 65). We found that the adhesion of sickle RBCs could be prevented by either anti-P-selectin or anti-Mac-1 antibody, indicating that both molecules contribute to the adhesion of sickle RBCs to the vascular endothelium. In our studies, blocking Mac-1 had a more pronounced effect on adhesion than did impairing P-selectin activity. The beneficial impact of interfering with Mac-1 in SCD has been supported by the reduction of RBC-neutrophil interaction in SCD mice treated with anti-Mac-1 Ab(51) or in Mac-1-

deficient SCD mice (57). Thus, our data indicates that complement is involved in the interaction between sickle RBCs and the endothelium, pointing to a new additional mechanism contributing to the biocomplexity of acute events in SCD.

Our study therefore has potential implications for the clinical management of SCD. Current treatments in development are focused on the role of selectins in SCD pathology. For example, the anti-P-selectin antibody (crizanlizumab) that has been used to treat SCD and it has been reported to affect the length of time between acute pain-crisis in SCD patients (52, 66, 67). Similarly, the small molecule-based pan-selectin inhibitor, rivipansel, currently undergoing phase 3 clinical trials, is able to reduce the time required to resolve vaso-occlusive crises with a reduction in opioid treatment (68). Our findings suggest that targeting complement opsonization and/or opsonin-mediated cell adhesion could provide an alternative strategy. Whereas, the use of exogenous full-length FH as a therapeutic tool is associated with some challenges for being used as a therapeutic, several smaller variants of the regulator have shown promise in preclinical trials for complement-mediated diseases such as PNH. Owing to the importance of FH domains 19-20 for interfering with RBC adhesion, mini-FH constructs containing this domain pair may be considered, since they may affect both AP activity and the adhesive function of existing opsonins (69, 70). Alternatively, blocking opsonization itself at the level of C3 activation is also expected to impair complement-mediated adhesion.

In conclusion, we have firstly shown that complement activation on sickle RBCs participates in the adhesion of sickle erythrocytes to the TNF-α activated vascular endothelium (Fig. 5B). We have further demonstrated that the FH19-20 segment is as efficient as FH in preventing the adhesion of sickle RBCs, and results in a normalization of sickle RBC transit across the vascular endothelial surface. We suggest that chronic hemolysis may require high levels of FH to prevent RBC adhesion and entrapment into microcirculation. Finally, our data indicate that FH might act as multimodal molecule, preventing the opsonization of sickle RBCs with C3 opsonins and targeting the interaction of sickle RBCs interaction with the endothelium through the adhesion molecules P-selectin and Mac-1 (Fig. 5B). Our findings provide a rationale for considering FH-based inhibitors and other modulators of the alternative complement pathway as potential new therapeutic options in SCD.

ACKNOWLEDGMENTS

This work was supported in part by grants by FUR 2016-2017 to L.DF and by NIH grant AI068730 to J.D.L. We thank Dr. Sara Ugolini, Dr. Monica Battiston and Dr. Francesco Agostini for technical support, Ing. Leoardo Buscemi for LB software writing and Ing. Vincenzo Insalaca for video editing. We thank Dr. Letizia Delmonte and Dr. Elisa Vencato for their contribution in preliminary experiments and Dr. Deborah McClellan for editing the manuscript.

AUTHORSHIP AND CONFLICT OF INTEREST

EL and AM carried out the experiments, analyzed the data and contributed to manuscript preparation; LDF, LDM, AMR, JDL, RD, and CC designed the experiments, analyzed the data and wrote the manuscript; MM contributed to manuscript preparation; DDZ developed the algorithm, analyzed data and contributed to manuscript preparation; SGL carried out the biochemical and the hematologic analyses; AS carried out experiments; CS carried out ELISA assays and contributed to data discussion; NM and OB carried out the statistical analyses, and FZ and ZB selected patients, collected blood samples and contributed to data discussion.

The authors report no conflict of interest.

REFERENCES

1. De Franceschi L, Cappellini MD, Olivieri O. Thrombosis and sickle cell disease. Semin Thromb Hemost. 2011;37(3):226-236.
2. Kato GJ, Hebbel RP, Steinberg MH, Gladwin MT. Vasculopathy in sickle cell disease: Biology, pathophysiology, genetics, translational medicine, and new research directions. Am J Hematol. 2009;84(9):618-625.
3. Hebbel RP. The systems biology-based argument for taking a bold step in chemoprophylaxis of sickle vasculopathy. Am J Hematol. 2009;84(9):543-545.
4. Parise LV, Telen MJ. Erythrocyte adhesion in sickle cell disease. Curr Hematol Rep. 2003;2(2):102-108.
5. De Franceschi L, Corrocher R. Established and experimental treatments for sickle cell disease. Haematologica. 2004;89(3):348-356.
6. Sabaa N, de Franceschi L, Bonnin P, et al. Endothelin receptor antagonism prevents hypoxia-induced mortality and morbidity in a mouse model of sickle-cell disease. J Clin Invest. 2008;118(5):1924-1933.

7. Vinchi F, De Franceschi L, Ghigo A, et al. Hemopexin therapy improves cardiovascular function by preventing heme-induced endothelial toxicity in mouse models of hemolytic diseases. Circulation. 2013;127(12):1317-1329.
8. Schaer DJ, Buehler PW, Alayash AI, Belcher JD, Vercellotti GM. Hemolysis and free hemoglobin revisited: exploring hemoglobin and hemin scavengers as a novel class of therapeutic proteins. Blood. 2013;121(8):1276-1284.
9. Hebbel RP. Adhesion of sickle red cells to endothelium: myths and future directions. Transfus Clin Biol. 2008;15(1-2):14-18.
10. Telen MJ. Beyond hydroxyurea: new and old drugs in the pipeline for sickle cell disease. Blood. 2016;127(7):810-819.
11. Risitano AM, Notaro R, Marando L, et al. Complement fraction 3 binding on erythrocytes as additional mechanism of disease in paroxysmal nocturnal hemoglobinuria patients treated by eculizumab. Blood. 2009;113(17):4094-4100.
12. Risitano AM, Notaro R, Pascariello C, et al. The complement receptor 2/factor H fusion protein TT30 protects paroxysmal nocturnal hemoglobinuria erythrocytes from complement-mediated hemolysis and C3 fragment. Blood. 2012;119(26):6307-6316.
13. Frimat M, Tabarin F, Dimitrov JD, et al. Complement activation by heme as a secondary hit for atypical hemolytic uremic syndrome. Blood. 2013;122(2):282-292.
14. Roumenina LT, Loirat C, Dragon-Durey MA, et al. Alternative complement pathway assessment in patients with atypical HUS. J Immunol Methods. 2011;365(1-2):8-26.
15. Test ST, Woolworth VS. Defective regulation of complement by the sickle erythrocyte: evidence for a defect in control of membrane attack complex formation. Blood. 1994;83(3):842-852.
16. Chudwin DS, Papierniak C, Lint TF, Korenblit AD. Activation of the alternative complement pathway by red blood cells from patients with sickle cell disease. Clin Immunol Immunopathol. 1994;71(2):199-202.
17. Wang RH, Phillips G, Jr., Medof ME, Mold C. Activation of the alternative complement pathway by exposure of phosphatidylethanolamine and phosphatidylserine on erythrocytes from sickle cell disease patients. J Clin Invest. 1993;92(3):1326-1335.
18. Mold C, Tamerius JD, Phillips G, Jr. Complement activation during painful crisis in sickle cell anemia. Clin Immunol Immunopathol. 1995;76(3 Pt 1):314-320.
19. Gavriilaki E, Mainou M, Christodoulou I, et al. In vitro evidence of complement activation in patients with sickle cell disease. Haematologica. 2017;102(12):e481-e482.
20. Koethe SM, Casper JT, Rodey GE. Alternative complement pathway activity in sera from patients with sickle cell disease. Clin Exp Immunol. 1976;23(1):56-60.
21. Strauss RG, Asbrock T, Forristal J, West CD. Alternative pathway of complement in sickle cell disease. Pediatr Res. 1977;11(4):285-289.
22. de Ciutiis A, Polley MJ, Metakis LJ, Peterson CM. Immunologic defect of the alternate pathway-of-complement activation postsplenectomy: a possible relation between splenectomy and infection. J Natl Med Assoc. 1978;70(9):667-670.
23. Schaid TR, Nguyen J, Chen C, et al. Complement activation in a murine model of sickle cell disease: inhibition of vaso-occlusion by blocking C5 activation. Blood. 2016;128(22):158.
24. Merle NS, Grunenwald A, Rajaratnam H, et al. Intravascular hemolysis activates complement via cell-free heme and heme-loaded microvesicles. JCI Insight. 2018;3(12).
25. Zipfel PF, Skerka C. Complement regulators and inhibitory proteins. Nat Rev Immunol. 2009;9(10):729-740.

26. de Cordoba SR, de Jorge EG. Translational mini-review series on complement factor H: genetics and disease associations of human complement factor H. Clin Exp Immunol. 2008;151(1):1-13.
27. Kajander T, Lehtinen MJ, Hyvarinen S, et al. Dual interaction of factor H with C3d and glycosaminoglycans in host-nonhost discrimination by complement. Proc Natl Acad Sci U S A. 2011;108(7):2897-2902.
28. Ricklin D, Reis ES, Lambris JD. Complement in disease: a defence system turning offensive. Nat Rev Nephrol. 2016;12(7):383-401.
29. Wu J, Wu YQ, Ricklin D, et al. Structure of complement fragment C3b-factor H and implications for host protection by complement regulators. Nat Immunol. 2009;10(7):728-733.
30. Morgan HP, Schmidt CQ, Guariento M, et al. Structural basis for engagement by complement factor H of C3b on a self surface. Nat Struct Mol Biol. 2011;18(4):463-470.
31. Dworkis DA, Klings ES, Solovieff N, et al. Severe sickle cell anemia is associated with increased plasma levels of TNF-R1 and VCAM-1. Am J Hematol. 2011;86(2):220-223.
32. Magro CM, Momtahen S, Mulvey JJ, et al. Role of the skin biopsy in the diagnosis of atypical hemolytic uremic syndrome. Am J Dermatopathol. 2015;37(5):349-356; quiz 357-349.
33. Scambi C, Ugolini S, Jokiranta TS, et al. The local complement activation on vascular bed of patients with systemic sclerosis: a hypothesis-generating study. PLoS One. 2015;10(2):e0114856.
34. Vianello A, Vencato E, Cantini M, et al. Improvement of maternal and fetal outcomes in women with sickle cell disease treated with early prophylactic erythrocytapheresis. Transfusion. 2018;58(9):2192-2201.
35. de Jong K, Emerson RK, Butler J, et al. Short survival of phosphatidylserine-exposing red blood cells in murine sickle cell anemia. Blood. 2001;98(5):1577-1584.
36. de Jong K, Larkin SK, Styles LA, Bookchin RM, Kuypers FA. Characterization of the phosphatidylserine-exposing subpopulation of sickle cells. Blood. 2001;98(3):860-867.
37. de Franceschi L, Turrini F, Honczarenko M, et al. In vivo reduction of erythrocyte oxidant stress in a murine model of beta-thalassemia. Haematologica. 2004;89(11):1287-1298.
38. Hebbel RP. Adhesive interactions of sickle erythrocytes with endothelium. J Clin Invest. 1997;100(11 Suppl):S83-86.
39. Montes RA, Eckman JR, Hsu LL, Wick TM. Sickle erythrocyte adherence to endothelium at low shear: role of shear stress in propagation of vaso-occlusion. Am J Hematol. 2002;70(3):216-227.
40. Barabino GA, McIntire LV, Eskin SG, Sears DA, Udden M. Endothelial cell interactions with sickle cell, sickle trait, mechanically injured, and normal erythrocytes under controlled flow. Blood. 1987;70(1):152-157.
41. Jokiranta TS, Hellwage J, Koistinen V, Zipfel PF, Meri S. Each of the three binding sites on complement factor H interacts with a distinct site on C3b. J Biol Chem. 2000;275(36):27657-27662.
42. Matte A, De Falco L, Federti E, et al. Peroxiredoxin-2: A Novel Regulator of Iron Homeostasis in Ineffective Erythropoiesis. Antioxid Redox Signal. 2018;28(1):1-14.
43. Elmariah H, Garrett ME, De Castro LM, et al. Factors associated with survival in a contemporary adult sickle cell disease cohort. Am J Hematol. 2014;89(5):530-535.

44. Kalambur VS, Mahaseth H, Bischof JC, et al. Microvascular blood flow and stasis in transgenic sickle mice: utility of a dorsal skin fold chamber for intravital microscopy. Am J Hematol. 2004;77(2):117-125.
45. Vercellotti GM, Zhang P, Nguyen J, et al. Hepatic Overexpression of Hemopexin Inhibits Inflammation and Vascular Stasis in Murine Models of Sickle Cell Disease. Mol Med. 2016;22.
46. Serjeant GR. Leg ulceration in sickle cell anemia. Arch Intern Med. 1974;133(4):690-694.
47. Yawn BP, Buchanan GR, Afenyi-Annan AN, et al. Management of sickle cell disease: summary of the 2014 evidence-based report by expert panel members. JAMA. 2014;312(10):1033-1048.
48. Matsui NM, Borsig L, Rosen SD, et al. P-selectin mediates the adhesion of sickle erythrocytes to the endothelium. Blood. 2001;98(6):1955-1962.
49. Manwani D, Frenette PS. Vaso-occlusion in sickle cell disease: pathophysiology and novel targeted therapies. Blood. 2013;122(24):3892-3898.
50. Wood K, Russell J, Hebbel RP, Granger DN. Differential expression of E- and P-selectin in the microvasculature of sickle cell transgenic mice. Microcirculation. 2004;11(4):377-385.
51. Hidalgo A, Chang J, Jang JE, et al. Heterotypic interactions enabled by polarized neutrophil microdomains mediate thromboinflammatory injury. Nat Med. 2009;15(4):384-391.
52. Ataga KI, Kutlar A, Kanter J. Crizanlizumab in Sickle Cell Disease. N Engl J Med. 2017;376(18):1796.
53. Cherqui S, Kurian SM, Schussler O, et al. Isolation and angiogenesis by endothelial progenitors in the fetal liver. Stem Cells. 2006;24(1):44-54.
54. Aranguren XL, Agirre X, Beerens M, et al. Unraveling a novel transcription factor code determining the human arterial-specific endothelial cell signature. Blood. 2013;122(24):3982-3992.
55. Lotzer K, Dopping S, Connert S, et al. Mouse aorta smooth muscle cells differentiate into lymphoid tissue organizer-like cells on combined tumor necrosis factor receptor-1/lymphotoxin beta-receptor NF-kappaB signaling. Arterioscler Thromb Vasc Biol. 2010;30(3):395-402.
56. Del Conde I, Cruz MA, Zhang H, Lopez JA, Afshar-Kharghan V. Platelet activation leads to activation and propagation of the complement system. J Exp Med. 2005;201(6):871-879.
57. Chen G, Chang J, Zhang D, et al. Targeting Mac-1-mediated leukocyte-RBC interactions uncouples the benefits for acute vaso-occlusion and chronic organ damage. Exp Hematol. 2016;44(10):940-946.
58. Kassebaum NJ, Jasrasaria R, Naghavi M, et al. A systematic analysis of global anemia burden from 1990 to 2010. Blood. 2014;123(5):615-624.
59. Ricklin D, Reis ES, Mastellos DC, Gros P, Lambris JD. Complement component C3 - The "Swiss Army Knife" of innate immunity and host defense. Immunol Rev. 2016;274(1):33-58.
60. Beller DI, Springer TA, Schreiber RD. Anti-Mac-1 selectively inhibits the mouse and human type three complement receptor. J Exp Med. 1982;156(4):1000-1009.

61. De Franceschi L, Franco RS, Bertoldi M, et al. Pharmacological inhibition of calpain-1 prevents red cell dehydration and reduces Gardos channel activity in a mouse model of sickle cell disease. FASEB J. 2013;27(2):750-759.
62. Stocker JW, De Franceschi L, McNaughton-Smith GA, et al. ICA-17043, a novel Gardos channel blocker, prevents sickled red blood cell dehydration in vitro and in vivo in SAD mice. Blood. 2003;101(6):2412-2418.
63. de Franceschi L, Baron A, Scarpa A, et al. Inhaled nitric oxide protects transgenic SAD mice from sickle cell disease-specific lung injury induced by hypoxia/reoxygenation. Blood. 2003;102(3):1087-1096.
64. Saggu G, Cortes C, Emch HN, et al. Identification of a novel mode of complement activation on stimulated platelets mediated by properdin and C3(H2O). J Immunol. 2013;190(12):6457-6467.
65. Atkinson C, Zhu H, Qiao F, et al. Complement-dependent P-selectin expression and injury following ischemic stroke. J Immunol. 2006;177(10):7266-7274.
66. Ataga KI, Kutlar A, Kanter J, et al. Crizanlizumab for the Prevention of Pain Crises in Sickle Cell Disease. N Engl J Med. 2017;376(5):429-439.
67. Slomski A. Crizanlizumab Prevents Sickle Cell Pain Crises. JAMA. 2017;317(8):798.
68. Telen MJ, Wun T, McCavit TL, et al. Randomized phase 2 study of GMI-1070 in SCD: reduction in time to resolution of vaso-occlusive events and decreased opioid use. Blood. 2015;125(17):2656-2664.
69. Harder MJ, Anliker M, Hochsmann B, et al. Comparative Analysis of Novel Complement-Targeted Inhibitors, MiniFH, and the Natural Regulators Factor H and Factor H-like Protein 1 Reveal Functional Determinants of Complement Regulation. J Immunol. 2016;196(2):866-876.
70. Nichols EM, Barbour TD, Pappworth IY, et al. An extended mini-complement factor H molecule ameliorates experimental C3 glomerulopathy. Kidney Int. 2015;88(6):1314-1322.

Table 1. Demographic, hematologic and biochemical data for healthy subjects and SCD patients

Parameters	Healthy Subjects (*n*= 29)	SCD Patients (*n=29)*
Age (yr)	30.0 (25.0-42.5)	**20.0 (17.0-47.0)***
Gender (M/F) (*n*)	11/18	10/19
Smokers (%)	10.3% (3)	6.8% (2)
Systolic blood pressure (mmHg)	120 (110-130)	120 (112-130)
Dyastolic blood pressure (mmHg)	65 (58-77)	64 (60-76)
Hb (g/dL)	13.4 (12.5)	**8.5 (8-9.5) ***
HbF (%)	2 (1.8-2.1)	**4.5 (2.5-7.6) ***
Reticulocytes (cells * 10^3/uL)	44.6 ±12	**250 ±27***
White blood cells (10^9 cells/μL)	4.5 (3.8-5.2)	**10.2 (8.8-11.9)**
Creatinine (mg/dL)	0.8 (0.7-1.0)	0.7 (0.3-1.5)
LDH (U/L)	325.0 (261.5-413.0)	**484.0 (310.2-1104.2) ***
Albumin (g/L)	42.3 (39.2-46.7)	44.3 (35.6-49.7)
CRP (mg/L)	0.9 (0.2-12.4)	**3.0 (1.0-15.8) ***
sVCAM-1 (pg/mL)	280 ±14	**820±36***

Yr: year; M: male; F: female; Hb: hemoglobin; HbF: fetal hemoglobin; LDH: lactate dehydrogenase; CRP: C reactive protein; sVCAM-1: serum vascular adhesion molecule-1. Ranges are shown in parentheses.

FIGURE LEGENDS

Fig. 1. The adhesion of C3d+ sickle RBCs is prevented by Factor H. (A) Healthy control (AA) and sickle cell (SCD) plasma samples were tested by ELISA assay (see Methods section); *p<0.05 AA *vs* SCD; *n*=10 in each group. **(B)** Deposition of C5b-9 (orange fluorescence) assessed by immunofluorescent staining involving the abluminal aspect of the microvasculature in apparently normal skin of an SCD patient (direct immunofluorescence; original magnification x100). **Inset**. Detail of the vessels showing intense granular deposition of C5b9; direct immunofluorescence; original magnification: x 400. Nuclei were stained with Prolong Gold antifade reagent with DAPI (blue fluorescence). The image shown is one representative image of other 16 with similar results. **Lower panel.** The percentage of vessels positive (+) for C5b9 granular deposition in skin biopsies from healthy (AA) and sickle cell patients (SCD). Data are shown as means±SD **p<0.002 AA *vs* SCD. **(C) Left panel.** Representative immunohistochemical image of a normal skin biopsy from SCD patient, showing a small vessel in the superficial dermis (arrow) characterized by co-expression of C5b9 (brown) and CD31 (red); for comparison a C5b9 negative vessel (circle) only decorated with CD31 staining (red) is highlighted. One representative image is shown; all 16 gave similar results (n=16). **Right panel.** Quantification of C5b9 positive vessels in skin biopsies from health (see Fig. 2S) and SCD patients. Data are shown as means ±SD; **p<0.01 AA vs SCD.
(D) Percentage of C3d positive red cell (red blood cells, RBCs) (C3d+) in healthy donor (AA) and in sickle cell subjects (*n*=16 AA; *n*=16 SCD). The dashed line indicates the threshold of normality, corresponding to C3d+ <0.5 % of RBCs; *p<0.05 AA *vs* SCD; ** p < 0.01 AA *vs* SCD**. (E)** Percentage of phosphatydylserine (PS) positive red cell (red blood cells, RBCs) (PS+) in healthy donor (AA) and in sickle cell subjects (*n*=20 AA; *n*=32 SCD). The dashed line indicates the threshold of normality, corresponding to C3b+ <0.5 % of RBCs; ** p < 0.01 AA *vs* SCD.

Fig. 2. (A) Healthy (AA) or sickle cell (SCD) RBC adhesion on immortalized endothelium (EA926.hy) treated with or without TNF-α under flow conditions (data are expressed as cells/mm^2). Data are obtained from six separate comparable experiments. All calculations were performed using the IBM SPSS 20.0 (IBM Inc., Armonk, NY) statistical package. Adhesion tests are expressed as median values with the minimum-maximum range and shown by means of box plots. Data are analyzed with non-parametric tests, Mann-Whitney *U* test for unpaired samples and Wilcoxon signed-rank test for paired samples. A value of $P<0.05$ is considered statistically significant. **(B)** Dose-response curve for factor H (FH) in adhesion assay for healthy (AA) or sickle (SCD) red blood cells (RBCs). Data were obtained at 6 min flux on endothelium treated with either vehicle or TNF-α. The curve is representative of six separated and independent experiments with similar results.

Fig. 3. FH and FH19-20 segment normalized the transit of sickle RBCs on TNF-α activated vascular endothelial surface. (A) Sickle cell adhesion after 6 minutes of perfusion on activated or non-activated endothelium (+/- TNF-α) in the presence of FH 9 nM or 18nM final concentration. The data shown are representative of other six independent assays with similar results (*n*=6). Wilcoxon test: * indicates the corresponding significance. A value of $p<0.05$ was considered statistically significant. Statistical analysis as in Fig. 2A. **(B)** Sickle cell adhesion after 6 minutes of perfusion on activated or non-activated endothelium (+/- TNF-α) in presence of FH and its fragments 19-20 e 6-8 (18nM final concentration). Data shown are representative of other 6 independent assays with similar results (*n*=6). A value of $p<0.05$ was considered statistically significant. Statistical analysis as in Fig. 2A.

Fig. 4. FH and FH 19-20 fragment normalized the "stop-and-go" motion of sickle RBCs. (A) Trajectory of three representative healthy RBCs in the field of view: each coordinate indicates their centroid at every consecutive frame (flow direction: x axis). (**B)** Trajectory of three representative sickle RBCs, showing the "stop-and-go" motion. (**C)** Trajectory of three representative sickle RBCs treated with FH (18 nM). **(D)** Trajectory of three representative sickle RBCs treated with FH 19-20 segment (18 nM). **(E)** Absolute values for instantaneous transverse speed expressed as mean ± standard deviation (** $p < 0.01$ *vs* healthy RBCs).

Fig. 5. FH anti-adhesive effect involves P-selectin and Mac-1 pro-adhesive molecules. **(A)** Sickle cell adhesion after 6 minutes of perfusion on activated or non-activated endothelium (+/- TNF-α) pre-coated with either anti-P-selectin antibody or anti-Mac1 (CD11b/CD18) antibody. Data shown are representative of other 6 independent assays with similar results. Wilcoxon test: * indicates the corresponding significance. Adhesion is expressed as median values with a minimum-maximum range and shown by means of box plots. A value of $p<0.05$ was considered statistically significant. Statistical analysis as in Fig. 2A. **(B)** Schematic model of the beneficial action of Factor H in reducing adhesion of C3-derived opsonins sickle RBCs to the TNF-α activated vascular endothelium. C3 split-fragments on erythrocyte might favor cell-cell interactions through P-selectin and Mac-1. P-selectin might bind RBCs through two different targets iC3b and/or sialic acid; in contrast, Mac-1 targets only iC3b deposit on sickle RBCs as more selective interaction. FH and FH19-20 segment normalized the transit of sickle RBCs across the TNF-α activated vascular endothelial surface, abolishing the “stop-and-go” behavior of the sickle RBCs. This effect positively affected (shortened) the transit time of sickle RBCs, reducing the likelihood of the RBCs to sickle during their transit of the microcirculation.

Fig. 1

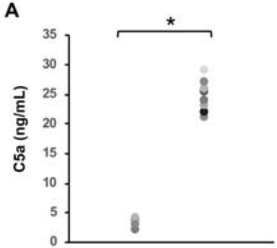
A
*
C5a (ng/mL)
35
30
25
20
15
10
5
0
AA
SCD

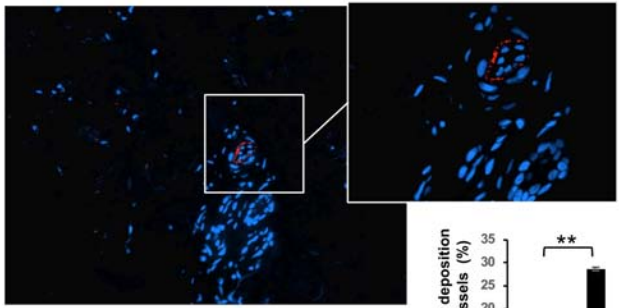
B
**
C5b9 granular deposition positive vessels (%)
35
30
25
20
15
10
5
0
AA
SCD

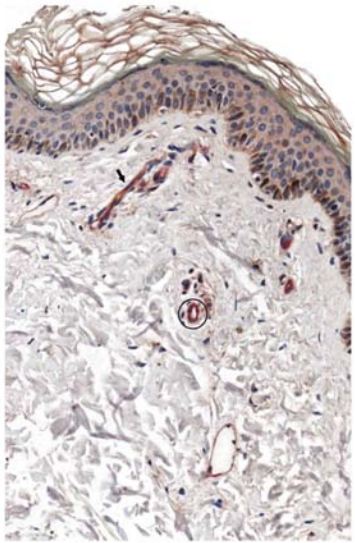
C

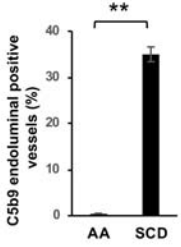
**
C5b9 endoluminal positive vessels (%)
40
30
20
10
0
AA
SCD

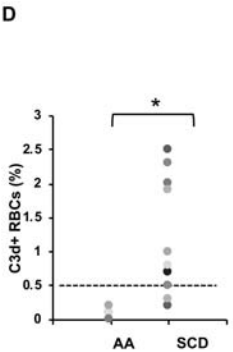
D
*
C3d+ RBCs (%)
3
2.5
2
1.5
1
0.5
0
AA
SCD

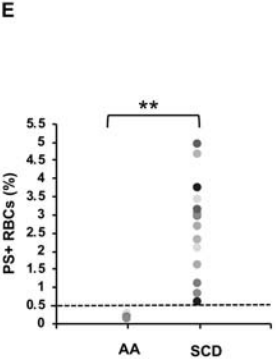
E
**
PS+ RBCs (%)
5.5
5
4.5
4
3.5
3
2.5
2
1.5
1
0.5
0
AA
SCD

Fig. 2

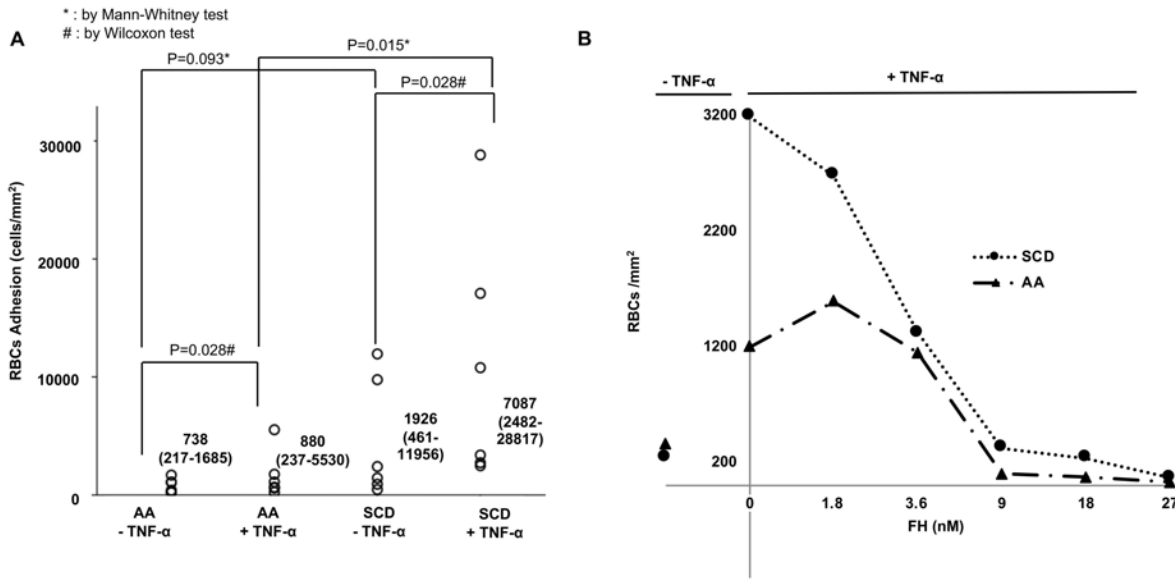
* : by Mann-Whitney test
# : by Wilcoxon test
A
P=0.093*
P=0.015*
P=0.028#
P=0.028#
RBCs Adhesion (cells/mm²)
30000
20000
10000
0
738
(217-1685)
880
(237-5530)
1926
(461-
11956)
7087
(2482-
28817)
AA
- TNF-α
AA
+ TNF-α
SCD
- TNF-α
SCD
+ TNF-α
B
- TNF-α
+ TNF-α
3200
2200
1200
200
RBCs /mm²
SCD
AA
0
1.8
3.6
9
18
27
FH (nM)

Fig. 3

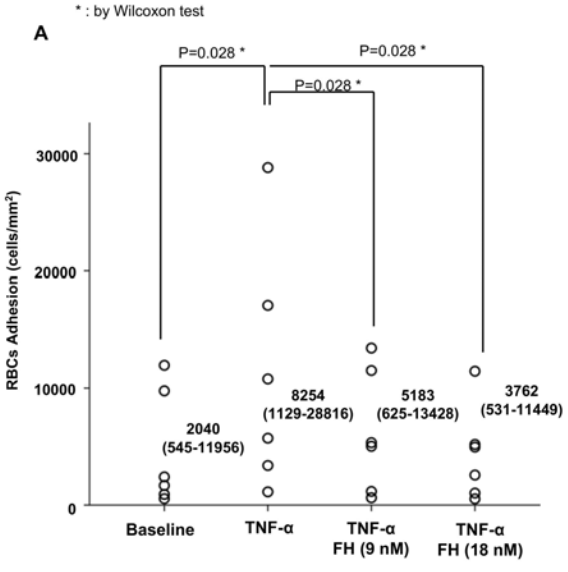
* : by Wilcoxon test
A
P=0.028 *
P=0.028 *
P=0.028 *
RBCs Adhesion (cells/mm²)
30000
20000
10000
0
2040
(545-11956)
8254
(1129-28816)
5183
(625-13428)
3762
(531-11449)
Baseline
TNF-α
TNF-α FH (9 nM)
TNF-α FH (18 nM)

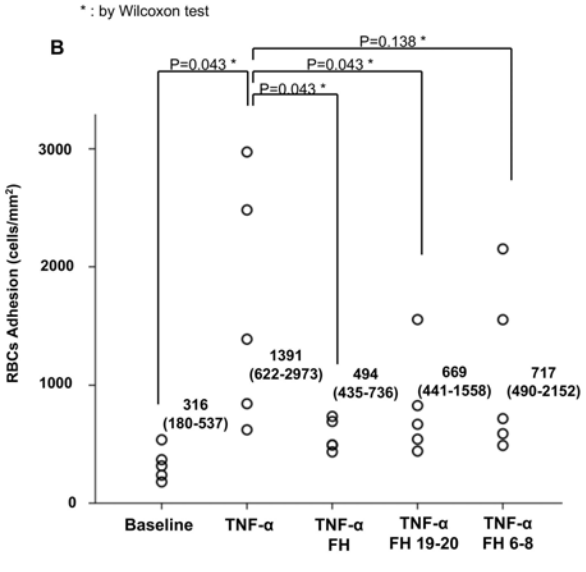
* : by Wilcoxon test
B
P=0.138 *
P=0.043 *
P=0.043 *
P=0.043 *
RBCs Adhesion (cells/mm²)
3000
2000
1000
0
316
(180-537)
1391
(622-2973)
494
(435-736)
669
(441-1558)
717
(490-2152)
Baseline
TNF-α
TNF-α FH
TNF-α FH 19-20
TNF-α FH 6-8

Fig. 4

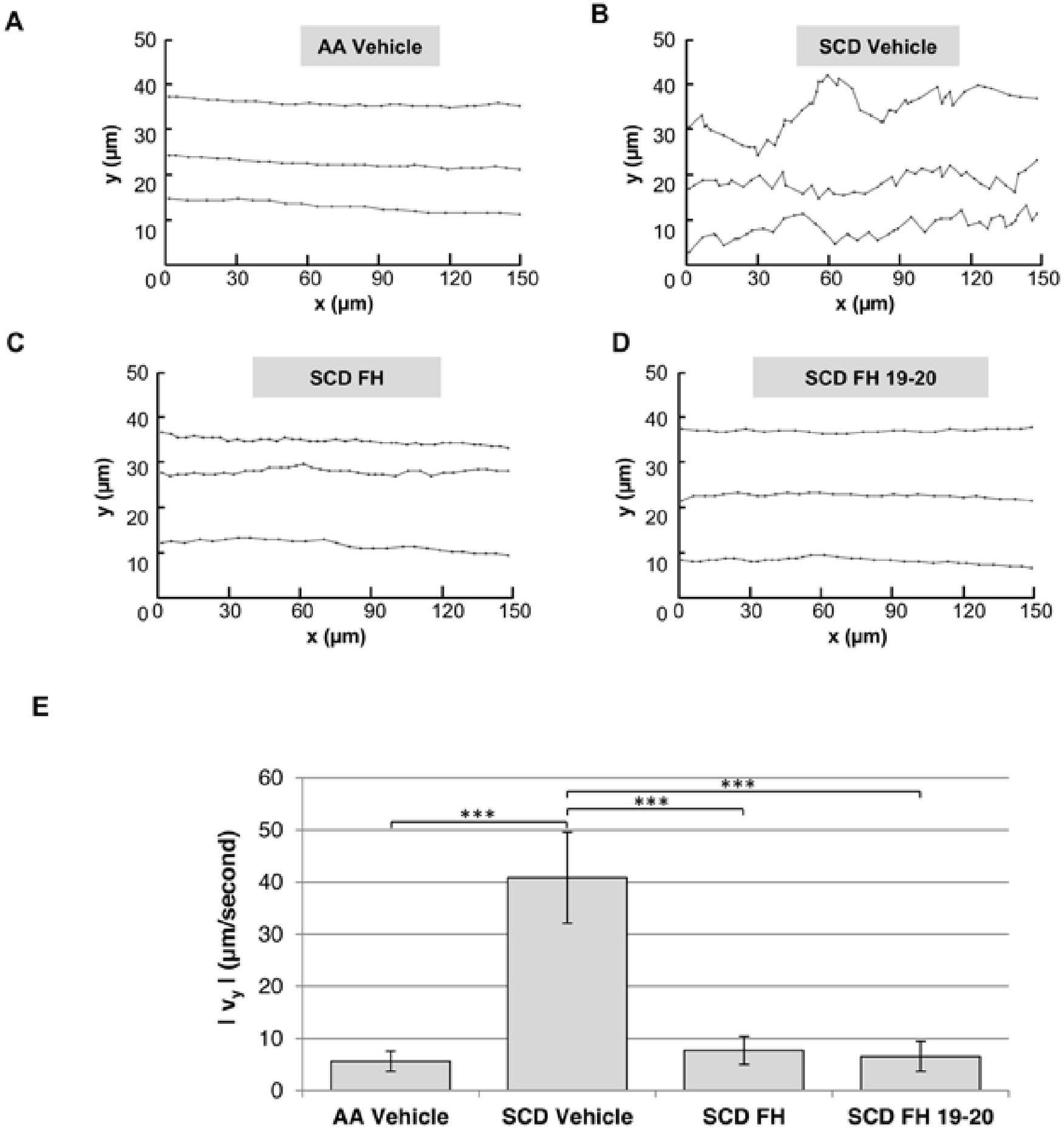
A
AA Vehicle
B
SCD Vehicle
C
SCD FH
D
SCD FH 19-20
y (µm)
x (µm)
0
10
20
30
40
50
0
30
60
90
120
150
E
| v_y | (µm/second)
60
50
40
30
20
10
0
***
***
***
AA Vehicle
SCD Vehicle
SCD FH
SCD FH 19-20

Fig. 5

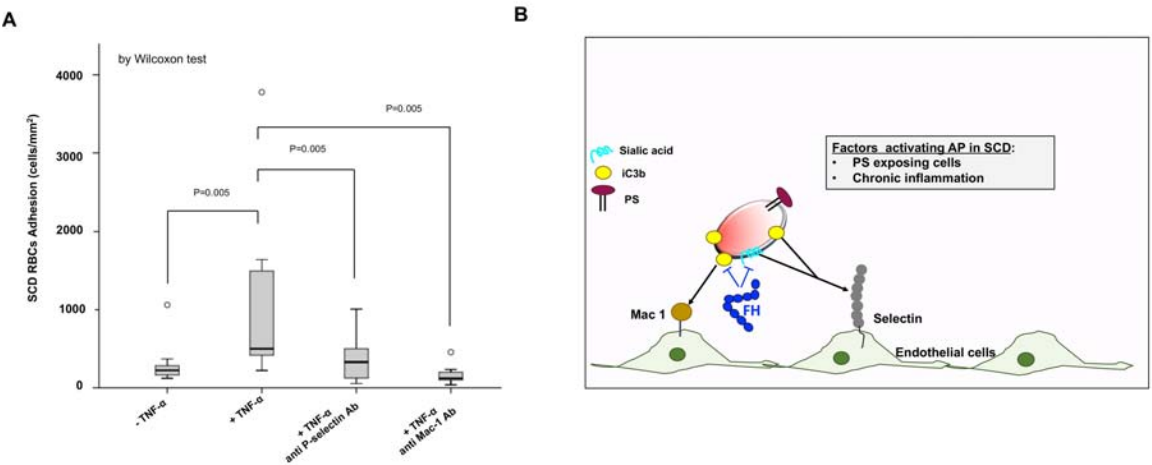
A
by Wilcoxon test
SCD RBCs Adhesion (cells/mm²)
4000
3000
2000
1000
0
P=0.005
P=0.005
P=0.005
- TNF-α
+ TNF-α
+ TNF-α anti P-selectin Ab
+ TNF-α anti Mac-1 Ab
B
Sialic acid
iC3b
PS
Factors activating AP in SCD:
• PS exposing cells
• Chronic inflammation
Mac 1
FH
Selectin
Endothelial cells

SUPPLEMENTARY FIGURES

Fig. 1S

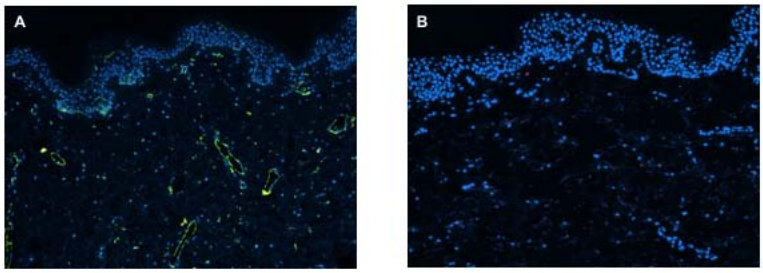

Fig. 1S. A. CD31 staining showing positive vessels (green fluorescence) in normal skin of control samples. Nuclei were stained with Prolong Gold antifade reagent with DAPI (blue fluorescence). Direct immunofluorescence; original magnification x 100. **B.** Serial section of the same subject showing negative C5b9 expression on microvasculature (orange fluorescence). Direct immunofluorescence; original magnification x 100. One representative image of other 16 with similar results.

Fig. 2S

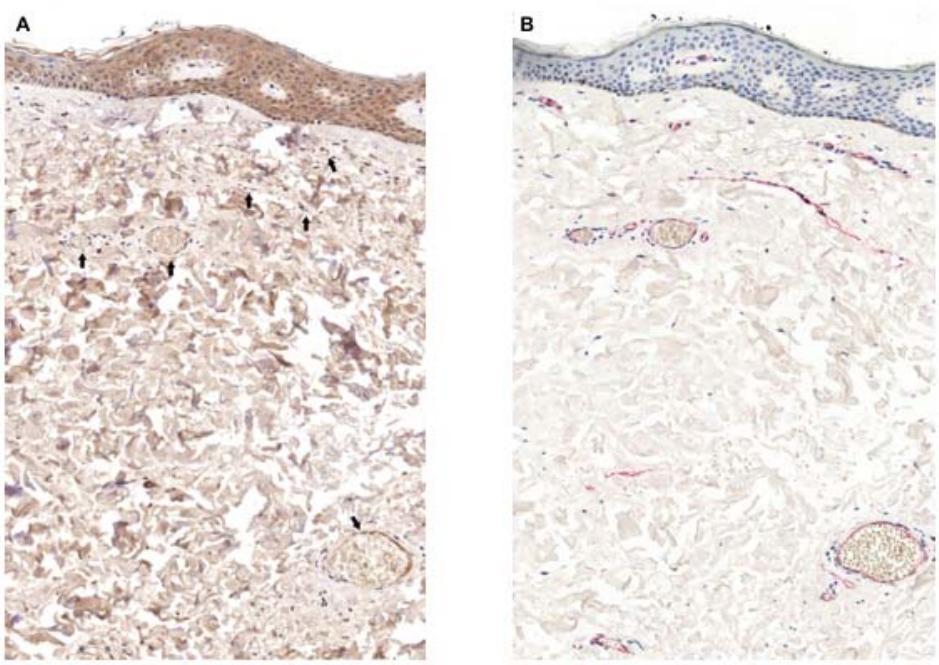

Fig. 2S. Representative immunohistochemical image of skin biopsy from healthy control, showing **(A)** all dermal vessel completely negative for C5b9 (arrow) and **(B)** the presence of vessels highlighted with CD31 staining (red) on the same field of panel A, from a consecutive histological section.

Fig. 3S

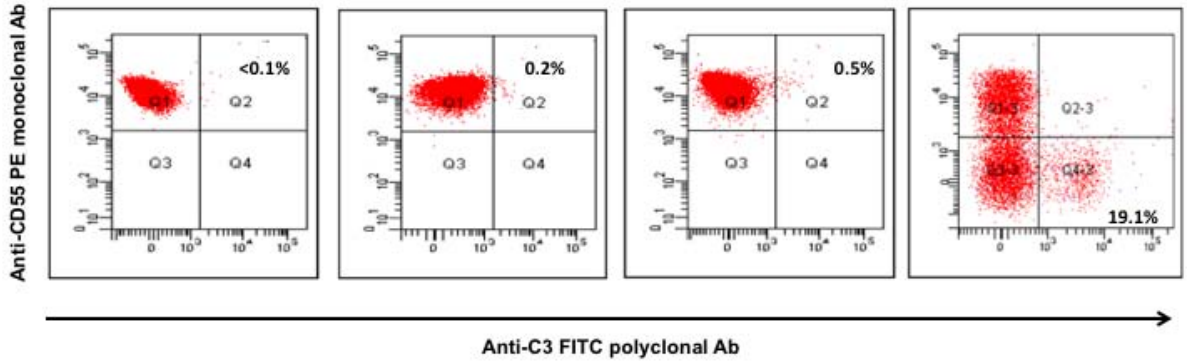

Fig. 3S. Flow cytometry of red blood cells from (from the left to the right): i. healthy subject (negative control); ii. and iii. sickle cell disease (SCD) patients; iv. paroxysmal nocturnal hemoglobinuria (PNH) patient on eculizumab (Risitano et al, Blood 2009). In each scatter-plot graph quadrants from Q1 to Q4 (Q1-1 to Q1-4 for the PNH patients, only viable erythrocytes are gated) represent respectively CD59+/c3-, CD59+/C3+, CD59-/C3- and CD59-/C3+ red blood cells. In healthy individuals, only CD59+/C3- cells are found (negative control); in PNH (positive control) a large population of C3+ cells is found, but only within the CD59- (PNH) red cell population (i.e., CD59-/C3+ cells). In SCD, a small population of C3+ cells is found, of course within CD59+ cell (no CD59, PNH-like cell can be detected).One representative of independent experiments with similar results; all data are presented in Fig. 1 scatter-plot graph.

Fig. 4S

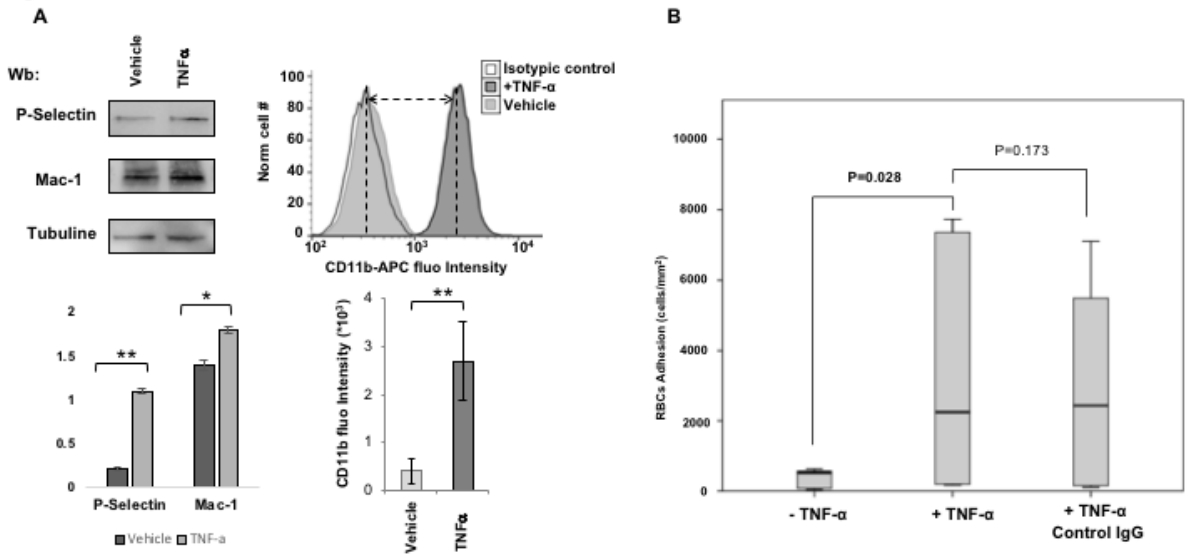

Fig. 4S. A. Western-blot (Wb) analysis of P-selectin and MAC-1 on activated (TNF-α) or non-activated vascular endothelium cells (Vehicle). Tubulin was used as protein loading control. **Lower panel.** Densitometric analyses of the immunoblot bands similar to those shown are presented at right (DU: densitometric Unit). Data are shown as means ±SD (*n*=3; *p<0.05; **p<0.02 compared to Vehicle). **Right panel**. Flow cytometry of activated (TNF-α) or non-activated vascular endothelium cells (Vehicle) stained with CD11b. Isotopic control is shown. One representative of 3 independent experiments with similar results.**(bottom**) Data are presented as means±SD (n=3; ; **p<0.02 compared to Vehicle).

B. Sickle red blood cell adhesion after 6 minutes of perfusion on activated or non-activated endothelium (+/- TNF-α) pre-coated with either vehicle or control IgG2 anti aCD20 antibody. Data shown are representative of other 6 independent assays with similar results. Wilcoxon test: * indicates the corresponding significance. All calculations were performed using the IBM SPSS 20.0 (IBM Inc., Armonk, NY) statistical package. Adhesion is expressed as median value with minimum-maximum range and shown by means of box plots. Data were analyzed with non-parametric tests, Mann-Whitney *U* test for unpaired samples and Wilcoxon signed-rank test for paired samples. A value of P<0.05 was considered statistically significant.

SUPPLEMENTAL METHODS

Evaluation of C5b-9 complement deposition on fixed skin biopsy

Immunofluorescent staining assay. Paraffin-embedded tissue blocks were cut into 2 to 3 μm sections and mounted on adhesion microscope glass slides. After the sections were dewaxed and rehydrated. Antigen retrieval was performed in prewarmed citrate buffer (pH 6, at 95°C) for 30 minutes. The sections were cooled to room temperature and then incubated with a protein-blocking serum free solution for 15 minutes at room temperature (RT) to block non-specific binding. In healthy controls, we stained dermal vessels in serial sections by anti-CD31 as an endothelial marker (mouse monoclonal antibody at 1: 50 dilution, Clone JC70A, Dako, Denmark; green fluorescence) and C5b9 (anti-human SC5b-9 at 1:100 dilution; Quidel, San Diego, CA; orange fluorescence) staining in healthy controls (Figure 1SA). Since Sprott et al. previously reported C5b9 deposition to be detectable only in the vessel walls of pathologic skin with no involvement of other cutaneous compartments, we also analyzed anti-C5b9 staining in skin biopsies from SCD patients (32, 33). Slides were then incubated with the corresponding Alexa 488-conjugated antibody or Alexa 546-coniugated antibody (1:800; INVITROGEN Molecular Probes). Nuclei were stained with Prolong Gold antifade reagent with DAPI (INVITROGEN Molecular Probes, blue staining). Slides were examined with an Olympus BX61 microscope.

Immunohistochemical staining assay. Paraffin-embedded tissue blocks were cut into 2-3 μm sections and mounted on adhesion microscope glass slides. For immunohistochemical staining, sections were stained in an auto-stainer Leica Bond System with anti-C5b9 (AbCam clone aE11) and CD31(mouse monoclonal antibody at 1: 50 dilution, Clone JC70A, Dako, Denmark) as previously reported (34).

Measurements of phosphatidylserine+ and C3d+ RBCs

The deposition of C3-derived opsonins (i.e. C3b, iC3b, C3dg) on RBCs was measured by flowcytometry using an antibody (monoclonal antibody anti C3 - EIA Quidel Corp., San Diego, CA; USA) recognizing the C3d fragment and is reported as C3d+ cells (11, 12). In brief, RBCs were obtained from fresh peripheral blood after centrifugation and three washings in saline buffer; washed RBCs were resuspended in saline at approximately at the concentration of 10^4 RBCs/μL, and then incubated with a phycoerythrin (PE)–conjugated anti-CD59 (59PE Valter Occhiena) diluted 1:10, and with a fluorescein isothiocyanate (FITC)–conjugated anti-C3 polyclonal

antibody (Ab14396 Abcam; a 1:20 working solution from the original tube was used at a final dilution of 1:50). Samples were incubated at RT for 1 hour, and then analyzed with a FACScan cytometer (Becton Dickinson Italia), after dilution with 10 volumes of saline (or FACS flow, Becton Dickinson Italia).

Red blood cell adhesion assay

Blood samples were collected in ACD anticoagulant and RBCs were separated from the plasma, washed in phosphate buffer (PBS), re-suspended at 2% haematocrit (Hct) in RMPI serum-free Roswell Park Memorial Institute medium (RPMI, Gibco) medium (containing 1% bovine serum albumin, Sigma Aldrich), and then were incubated with 70uM Carboxyfluorescein Diacetate Succinimidyl Ester (CFDA-S; Life Technology) for 1 hour at 37°C. Labelled RBCs first were washed three times and then were re-suspended at 0.2% Hct in serum-free RMPI medium, containing 1% bovine serum albumin. The RBCs suspension, depleted of white blood cells (WBC), was then incubated for 10 minutes at 37°C with either full-length FH or its recombinant segments encompassing domains 6-8 (FH6-8) or 19-20 (FH19-20), which were produced as previously described (41), or with calcium and magnesium-free PBS as a negative control, then perfused to generate a wall shear stress of 30 sec^{-1}. Prior to the adhesion assays, haemolysis was determined using CN-FREE HGB reagent on ADVIA 120/2120 system (Siemens); no hemolysis was detected after the incubation time, prior to the adhesion assay (data not shown). A monolayer of immortalized endothelial cells (EA 926.hy cell line, ATCC® CRL-2922™) was grown at the bottom of the perfusion chamber, then incubated with TNFα (Sigma Aldrich-Merk KGaA, Darmstadt, Germany) for 4 hours at 37°C in 5% CO_2 in serum free medium. In preliminary experiments, primary TNFα-activated endothelial cells (HUVEC, ATCC® CRL-1730™) were used in the presence or absence of Factor H, and the results obtained were similar to those obtained with immortalized cells. RBC suspension perfused in the flow chamber was monitored for 10 minutes, during which time 10 different locations along a line oriented to the flow were examined every 3 min. in order to study cell adhesion and aggregation. To discriminate and count cells on flow we set-up a new software called Cell Counter-BL The software exploits the characteristics of long exposure photographs, in which the moving parts tend to disappear, while the adhering cells are imprinted on the image. Blocking antibodies against P-selectin (Anti-CD62P [AK4]; Abcam) or Mac-1 (CD11b/ CD18 [CBRM1/5]; Biolegend) were used at final concentration of 25 ug/ml.

Immortalized human endothelial cell EA926.hy were grown as monolayer in DMEM 10% FCS medium. This cell line was obtained from HUVEC (Human Umbelical Vein endothelial cell) cell line and maintain key characteristic of HUVEC. Endothelial cell passage was accomplished with trypsinization, as required. For flow experiments EA 926.hy cells were plated at a density sufficient to reach confluence. EA 926.hy cells were treated with 20nM TNFα for 4hours at 37 °C to create a cytokine mediated activation mimicking inflammatory state, non-activated endothelium was used as a control. In some experiment HUVEC cells were used as a control to compared and confirm results obtained with immortalized endothelial cells.

Flow chamber position and optical area of analysis

The flow chamber was positioned on the stage of an inverted microscope equipped with epifluorescent illumination (Diaphot-TMD; Nikon Instech, Shinagawa-ku, Japan), an intensified CCD videocamera (C-2400-87; Hamamatsu Photonics, Shizuoka, Japan), and appropriate filters. The total area of an optical field corresponded to approximately 0.007 mm^2. Blood cells were aspirated through the chamber with a syringe pump (Harvard Apparatus, Hollistone, MA) at a flow rate calculated to obtain the desired wall shear rate at the inlet. Experiments were recorded in real time on videotape at the rate of 25 frames/s, which resulted in a time resolution of 0.04 s.

Quantification of red blood cell adhesion: Cell Counter-BL Software

It is based on computational sum of frames that constitute a field of view. This is then divided by the number of frames obtaining an effect similar to a long exposure. The first image has non-homogeneous light background because of presence of a bright spot. For this reason, it was necessary to perform a background subtraction by calculation of the dynamic background on each image. An interpolating function of degree 4 was applied for all rows of the image. For the part of the cell count has exploited an algorithm known in the literature (http://en.wikipedia.org/wiki/Flood_fill).

Development of an algorithm to determine RBC transit and flux trajectory

Experiments were performed on an inverted fluorescence microscope and recorded in real time on videotape at the rate of 25 frames/second, resulting in a time resolution of 0.04 sec. Endothelial cells activated with TNFα were grown on the coverslip of the flow chamber and experiments were run as reported above. Selected video sequences were digitalized using VirtualDub software (www.virtualdub.org; open source software). Image analysis was accomplished using the Volocity software (Perkin Elmer) and by programming codes in MatLab R2014b (The

MathWorks). The trajectory of each individual RBC was followed with Volocity from first appearance of the particle in the field of view to its disappearance, considering the field in question as a fixed region of 125 x 375 pixels, which was equivalent to an area of 50 x 150 μm, (using a conversion factor of 0.4 μm/pixel).

For each RBC, fixing the x axis as the flow direction and the y axis as its perpendicular coordinate, the absolute values for instantaneous speed ($| v |_{t)}$ and for the instantaneous transverse speed ($| v_y |_{t,}$ both in μm/second) were quantified with MatLab, according to their definition, as:

$$| v |_t = \text{sqrt} (v_x^2 + v_y^2)_t = \text{sqrt} ((\Delta x / \Delta t)^2 + (\Delta y / \Delta t)^2)_t$$

$$| v_y |_t = | \Delta y / \Delta t |_t = | (y_t - y_{t-1}) / (t - (t-1)) |$$

where t is the time instant in which the calculation was performed and t-1 the preceding instant before. All computational analyses were performed frame by frame, for each observation time.

P-selectin and Mac-1 expression *in vitro* in vascular endothelial cells

Immunoblot analyses. Vascular endothelial cells were lysed with iced lysis buffer (LB containing: 150mMNaCl, 25mM bicine, 0.1% SDS, 2% Triton X-100, 1mM EDTA, protease inhibitor cocktail tablets [Roche] and 1mMNa_3VO_4 final concentration) followed by centrifugation at 4°C for 30 min at 12,000 g. Proteins were quantified and analyzed by mono-dimensional SDS polyacrylamide gel electrophoresis. Gels were transferred to nitrocellulose membranes for immunoblot analysis with specific antibodies: anti-P-Selectin (both from BD, Biosciences, San Jose, CA, USA)). Anti-tubulin was used as a loading control (Developmental Studies Hybridoma Bank [DSHB], Department of Biology, University of Iowa, Iowa City, IA, USA). Secondary donkey anti-rabbit IgG and HRP-conjugated were from GE Healthcare Life Sciences. Blots were developed by using the Luminata Forte Chemiluminescent HRP Substrate from Merck Millipore (Darmstadt, Germany), and images were acquired with an Image Quant Las Mini 4000 Digital Imaging System (GE Healthcare). Densitometric analyses were performed by using an ImageQuant TL software (GE Healthcare Life Sciences) (42).

Cytofluorimetric analysis. EA926.hy endothelial cells were seeded on a cover-sleep in order to obtain a cell monolayer. Endothelial cells were activated with

20ng/ml of TNFα in serum free medium for 4 hours before and then they were analyzed for surface CD11b (with anti MAC-1 APC, ICRF44 Biolegend). As controls, untreated cells and an isotypic antibody (MOPC-21 mouse IgG1k; Biolegend) were used. Analysis was performed with a FACScan cytometer (FORTESSA, Becton Dickinson).